

Overtaking Moving Obstacles with Digit: Path Following for Bipedal Robots via Model Predictive Contouring Control

Kunal S. Narkhede, Dhruv A. Thanki, Abhijeet M. Kulkarni and Ioannis Poulakakis

Abstract—Humanoid robots are expected to navigate in changing environments and perform a variety of tasks. Frequently, these tasks require the robot to make decisions online regarding the speed and precision of following a reference path. For example, a robot may want to decide to temporarily deviate from its path to overtake a slowly moving obstacle that shares the same path and is ahead. In this case, path following performance is compromised in favor of fast path traversal. Available global trajectory tracking approaches typically assume a given—specified in advance—time parametrization of the path and seek to minimize the norm of the Cartesian error. As a result, when the robot should be where on the path is fixed and temporary deviations from the path are strongly discouraged. Given a global path, this paper presents a Model Predictive Contouring Control (MPCC) approach to selecting footsteps that maximize path traversal while simultaneously allowing the robot to decide between faithful versus fast path following. The method is evaluated in high-fidelity simulations of the bipedal robot Digit in terms of tracking performance of curved paths under disturbances and is also applied to the case where Digit overtakes a moving obstacle.

I. INTRODUCTION

Consider a scenario in which a humanoid robot and a human share the same path with the human being in front of the robot but moving at a slower speed. The robot faces a decision between staying on the path—thus reducing its speed to avoid collisions with the human—or temporarily deviating from it to overtake the human. Global¹ path following approaches for humanoid robots cannot be used directly in such situations, because they typically require a pre-specified feasible time parametrization of the reference path, thus preventing the robot from deciding *online* when to be where on the path. Furthermore, these methods aim at maximizing path following accuracy, and hence do not permit temporary deviations that would result in faster path traversal. This paper describes a Model Predictive Control (MPC) approach with online time reparametrization of the reference path that enables bipedal robots to balance between maximizing path following accuracy versus fast path traversal.

A wide variety of methods have been proposed for planning motions with bipedal robots. Some methods require a collection of desired footsteps, e.g. [1], while others use reference velocity commands specified by a user [2]–[5] or by a kinematic model [6] and translate this information to

Center of Mass (COM) target trajectories using reduced-order models like the Linear Inverted Pendulum (LIP) [7]. Other methods take advantage of general sampling-based planning algorithms [8] to obtain global reference paths that are then approximately followed by the robot [9]–[11]. Obstacle-free paths in cluttered environments can also be constructed by switching among dynamic movement primitives with limit cycle equilibrium solutions [12]–[14], providing assured locomotion stability [15]. In the present paper, we turn our attention on path following, that is, on global position control, assuming that a sufficiently smooth reference global path is available *a priori*.

In the relevant literature, parametrizing a reference global path with respect to time is typically treated in isolation from the corresponding tracking problem. For example, [16], [17] provide a method for tracking a straight-line path under the assumption that a monotonically increasing, continuously differentiable time parametrization of the path is available *a priori*. Similarly, [18] assumes that a feasible time parametrization of the reference path is available in advance, and generates footsteps compatible with the resulting trajectory in a MPC fashion using a hybrid extension of the classical LIP [7]. However, decoupling the time parametrization of the path from the tracking problem may lead to inconsistencies between the resulting trajectory and the dynamics of the system. Furthermore, not allowing the robot to decide online when it should be where on the path may limit its ability to respond to changes in its surroundings.

Some methods do not assume a fixed time parametrization of the reference path. For instance [9] proposes a Quadratically Constrained Quadratic Program (QCQP) to modify the heading angle for a bipedal robot model by “shaping” a periodic walking gait computed offline so that a reference global path can be followed; however, in this work path traversal is primarily determined by the underlying periodic trajectory. Another approach proposed in [19] assumes a velocity profile along a reference path and converts it into walking patterns in the form of COM and Zero Moment Point (ZMP) trajectories; the velocity profile can be modified, but the ability to do this online is not explored. Translating a reference global path into a feasible COM trajectory is studied in [20], where part of the path is converted online into a trajectory by solving a direct collocation optimization problem using the Spring Loaded Inverted Pendulum (SLIP) model.

In this work, we assume that a path is given, and we adopt the approach in [21] and treat the path parameter as a state variable evolving according to a dynamical system. The input to this system is determined online via a MPC

K.S Narkhede, D. A. Thanki, A. M. Kulkarni, and I. Poulakakis are affiliated with the Department of Mechanical Engineering, University of Delaware, Newark, Delaware 19716, USA. {kunalnk, thankid, amkulk and poulakas}@udel.edu

This work was supported in part by NSF Award MRI-2018905.

¹The term “global” is used to refer to a path expressed with respect to an inertial frame of reference.

program and effectively decides how far into the path the robot goes in each step. This idea is at the core of Model Predictive Contouring Control (MPCC) [22], which combines online path reparametrization and tracking within a single optimization framework, the objective of which is to minimize the error to the reference path. The key aspect of the MPCC formulation is that the path following error is decomposed in *contouring* and *lag* components, allowing the system to assign different weights to maximizing tracking performance versus fast path traversal. This is different from the majority of the aforementioned methods [9], [11], [16]–[18], [20], which minimize the norm of the Cartesian error from the path, thus strongly penalizing deviations from it. MPCC has been implemented initially for tracing different contours in CNC machines [23], and more recently for path following and obstacle avoidance in wheeled robots [24] and for realizing aggressive flight maneuvers in quadrotors [25].

The goal of this paper is to enable bipedal robots to make decisions online regarding the speed and precision of following a reference global path. We propose a MPCC scheme that relies on a variant of the 3D LIP for footstep generation for bipedal robots. In contrast to previous work, our method does not require a fixed path parametrization in advance; the MPCC just needs a reference path, determines online a feasible (discrete) time parametrization, and suggests consistent footsteps and COM motions to the robot’s low-level controller. The latter is formulated as a Quadratic Program (QP) translating these suggestions to motor torques applied to the robot. The effectiveness of the method is evaluated in simulations with a high-fidelity model of the bipedal robot Digit². We discuss path following performance under randomly applied external disturbances, and demonstrate the application of the method to the case where Digit overtakes an obstacle moving along its path.

II. PATH FOLLOWING WITH ONLINE PARAMETRIZATION

We consider the problem of following a global path in the robot’s workspace. We describe in this section a method that allows for *online* time reparametrization of the path and discuss the selection of the performance index in a MPC program to enable the robot to decide between fast path traversal and path following performance.

A. Path Following MPC with Online Reparametrization

Consider a bipedal robot walking on flat ground. To keep the discussion general, assume that the step-to-step evolution of the robot can be predicted by a discrete-time system

$$\mathbf{x}_{k+1} = f(\mathbf{x}_k, \mathbf{u}_k) \quad (1)$$

where $\mathbf{x}_k \in \mathbb{R}^n$ and $\mathbf{u}_k \in \mathbb{R}^m$ are the state and input values of the system. Since we are interested in path following on the horizontal plane, we define the output

$$\mathbf{y}_k = h(\mathbf{x}_k) \quad (2)$$

where $\mathbf{y}_k = [x_k \ y_k]^\top \in \mathbb{R}^2$ is the location occupied by the robot at step k . In Section III below, we will adopt a

modified LIP as a prediction model (1)-(2) for the step-to-step dynamics of Digit.

We assume that a reference global path for the robot’s COM locations on the horizontal plane is available and that it can be represented as a sufficiently smooth curve

$$\mathbf{y}^d(\vartheta) = [x^d(\vartheta) \ y^d(\vartheta)]^\top \quad (3)$$

where the parameter $\vartheta \in \Theta = [0, \vartheta_T]$ measures “progress” along the path. Let

$$\phi^d(\vartheta) = \arctan \left(\frac{\partial y^d / \partial \vartheta}{\partial x^d / \partial \vartheta} \right) \Big|_{\vartheta} \quad (4)$$

be the slope of the path.

One way to discretize the path is to determine a fixed relationship between the step number k and the value of ϑ . This effectively corresponds to defining a trajectory $\mathbf{y}^d(\vartheta_k) = \mathbf{y}_k^d$ and the problem is equivalent to trajectory tracking: where the robot should be and when are specified. Instead, to allow the robot to decide *online* where on the path it should go at each step, we follow [21] and treat the path parameter ϑ as a state evolving according to the discrete dynamical system

$$\vartheta_{k+1} = \vartheta_k + v_k \quad (5)$$

in which v_k takes values in the interval $\mathcal{V} = [0, v_{\max}]$ and controls the progress of the robot along the path. In other words, the purpose of the update law (5) and its input v_k is to allow for reparametrizing the path online, effectively deciding how far into the path the robot travels at each step.

Given a path (3), the objective of the control system is to minimize the error between the current location $\mathbf{y}_k = h(\mathbf{x}_k)$ of the robot and the desired one specified by the parametrization $\mathbf{y}^d(\vartheta_k)$ of the path; that is, to minimize

$$\|e(\mathbf{x}_k, \vartheta_k)\|_Q^2 = (h(\mathbf{x}_k) - \mathbf{y}^d(\vartheta_k))^\top Q (h(\mathbf{x}_k) - \mathbf{y}^d(\vartheta_k))$$

where $Q = Q^\top > 0$ is a weighting matrix. In addition to minimizing the error, we wish to penalize input effort while maximizing progress along the path. These objectives can be captured by the running cost

$$J_1(\mathbf{x}_k, \vartheta_k, \mathbf{u}_k, v_k) = \|e(\mathbf{x}_k, \vartheta_k)\|_Q^2 + \|\mathbf{u}_k\|_R^2 - \rho |v_k|^2 \quad (6)$$

where $R = R^\top > 0$ and $\rho > 0$; the negative sign in the last term is to maximize how far into the path the robot goes at each step. Finally, the terminal cost is defined by

$$J_2(\mathbf{x}_{k+N}, \vartheta_{k+N}) = \|e(\mathbf{x}_{k+N}, \vartheta_{k+N})\|_W^2 \quad (7)$$

where $W = W^\top > 0$ is a weighting matrix.

With these definitions, path following can be realized by formulating a MPC over a finite horizon $N > 0$ as follows:

$$\begin{aligned} & \underset{X, U, V}{\text{minimize}} && \sum_{\ell=k}^{k+N-1} J_1(\mathbf{x}_\ell, \vartheta_\ell, \mathbf{u}_\ell, v_\ell) + J_2(\mathbf{x}_{k+N}, \vartheta_{k+N}) \\ & \text{subject to} && \mathbf{x}_k = \mathbf{x}_{\text{init}}, \quad \vartheta_k = \vartheta_{\text{init}} \\ & && \mathbf{x}_{\ell+1} = f(\mathbf{x}_\ell, \mathbf{u}_\ell), \quad \vartheta_{\ell+1} = \vartheta_\ell + v_\ell \\ & && \mathbf{x}_\ell \in \mathcal{X}_\ell, \quad \mathbf{u}_\ell \in \mathcal{U}_\ell, \quad \vartheta_\ell \in \Theta, \quad v_\ell \in \mathcal{V} \\ & && \mathbf{x}_{k+N} \in \mathcal{X}_{k+N}, \quad \vartheta_{k+N} \in \Theta \end{aligned}$$

²<https://www.agilityrobotics.com/robots#digit>

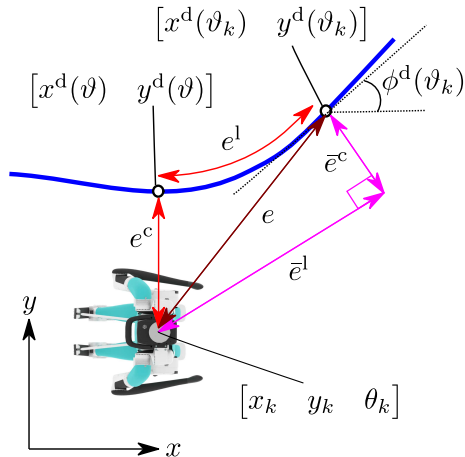


Fig. 1. Cartesian error e , and contouring e^c and lag e^l error components with their corresponding approximations \bar{e}^c and \bar{e}^l .

in which $\ell = k, \dots, k + N - 1$ and $X = \{x_{k+1}, \dots, x_{k+N}\}$, $U = \{u_k, \dots, u_{k+N-1}\}$, $V = \{v_k, \dots, v_{k+N-1}\}$. The sets $\mathcal{X}_k \subset \mathbb{R}^n$ and $\mathcal{U}_k \subset \mathbb{R}^m$ include permissible state³ and input values at step k , respectively. Given the reference path (3) and initial state x_{init} and path parameter ϑ_{init} , the MPC is solved at step k to provide an optimal sequence of inputs U^* . The first element u_k^* in this sequence is then applied at the robot and the process is repeated until the path is consumed.

B. Cartesian and Contouring Error Formulations

To motivate our discussion, note that a common way to select the weighting matrices Q and W in (6) and (7) is

$$Q = \alpha I \quad \text{and} \quad W = \beta I \quad (9)$$

where $\alpha > 0$, $\beta > 0$ and I is the identity matrix. This choice corresponds to minimizing the norm of the Cartesian error; see Fig. 1. However, it does not expose the tradeoff between accurately following the path and faithfully realizing the online—not a priori specified—time parametrization (5). As we will see in Section IV, making this tradeoff explicit is important in certain tasks, like overtaking moving obstacles.

To capture the interplay between the spatial and temporal aspects of tracking, we decompose the error as in [22] to *contouring* e^c and *lag* e^l components; see Fig 1. The contouring component captures the normal deviation from the path while the lag component measures the (path) distance that the robot lags behind the desired location $y^d(\vartheta_k)$. Since analytical expressions for e^c and e^l are not always available for general curved paths, these errors are approximated by \bar{e}^c and \bar{e}^l , respectively, (see Fig. 1), which are defined as

$$\bar{e}(x_k, \vartheta_k) = P(\phi^d(\vartheta_k))(h(x_k) - y^d(\vartheta_k))$$

where $\bar{e} = [\bar{e}^c \quad \bar{e}^l]^T$, $\phi^d(\vartheta_k)$ is the slope of the path at ϑ_k computed by (4) and

$$P(\phi^d(\vartheta_k)) = \begin{bmatrix} \sin(\phi^d(\vartheta_k)) & -\cos(\phi^d(\vartheta_k)) \\ -\cos(\phi^d(\vartheta_k)) & -\sin(\phi^d(\vartheta_k)) \end{bmatrix}.$$

³If there are obstacles in the output space and $\mathcal{Y}_k^{\text{free}}$ is the free part at step k , the state constraint $h(x_k) \in \mathcal{Y}_k^{\text{free}}$ determines in part the set \mathcal{X}_k .

With these definitions, the weighted running and terminal errors can be defined as

$$\|\bar{e}(x_k, \vartheta_k)\|_{\bar{Q}}^2 = \bar{e}(x_k, \vartheta_k)^T \bar{Q} \bar{e}(x_k, \vartheta_k)$$

$$\|\bar{e}(x_{k+N}, \vartheta_{k+N})\|_{\bar{W}}^2 = \bar{e}(x_{k+N}, \vartheta_{k+N})^T \bar{W} \bar{e}(x_{k+N}, \vartheta_{k+N})$$

respectively, which correspond to the cost functions (6) and (7) with weighting matrices selected according to

$$Q = P^T(\phi^d(\vartheta_k)) \bar{Q} P(\phi^d(\vartheta_k)) \quad (10)$$

$$W = P^T(\phi^d(\vartheta_k)) \bar{W} P(\phi^d(\vartheta_k)) \quad (11)$$

where

$$\bar{Q} = \text{diag}\{\alpha_1, \alpha_2\} \quad \text{and} \quad \bar{W} = \text{diag}\{\beta_1, \beta_2\} \quad (12)$$

are diagonal matrices with positive entries.

The selection of the weighting matrices according to (10)-(11) in the definition of the cost functions of the MPC program results in the MPCC formulation [22]. In what follows, we use the term MPCC to emphasize that the corresponding MPC program is formulated using the contouring/lag error decomposition. The advantage of splitting the error into contouring and lag components and using the weighting matrices (10) and (11) in (6) and (7) is that they provide explicit control over the normal deviation of the robot from the path. By choosing the entries in (12) one can prioritize between following the path accurately and keeping up with the underlying time parametrization. For example, in the case where Digit and a moving obstacle follow the same path with the obstacle being ahead of the robot, selecting $\alpha_1 = \alpha_2 = \alpha$ and $\beta_1 = \beta_2 = \beta$ results in the weighting matrices (9) causing the robot to limit its speed in order to stay on path while avoiding collisions. In this case, the obstacle sets the pace of the robot. On the other hand, selecting suitable values $\alpha_1 < \alpha_2$, and $\beta_1 < \beta_2$ causes the robot to prioritize fast traversal over path following, allowing it to temporarily deviate from the path to overtake the obstacle.

III. IMPLEMENTATION ON DIGIT

This section describes the 3D LIP model that will replace (1)-(2) as a prediction model in the MPC and discusses a QP controller for following the MPC suggestions.

A. Path Tracking MPC with LIP-based Predictions

1) *3D-LIP Model*: The LIP consists of a massless prismatic leg, on top of which is a point mass that is constrained to move in a horizontal plane located at height H ; see Fig. 2. Let (x, y) be the location of the point mass in the horizontal plane with respect to an inertial frame $\{X, Y, Z\}$ and let u^x and u^y be the distances between the ground contact point and the model's point mass along the X and Y axes, respectively. To ensure that the footstep locations suggested by the LIP do not violate the geometric constraints of Digit, we restrict the swing foot's feasible landing locations to lie within a rectangular region of orientation θ with respect to the Z axis, as shown in Fig. 2. We assume that θ is constant within each step and is updated instantaneously at the exchange of support by a step change u^θ ; see also [11].

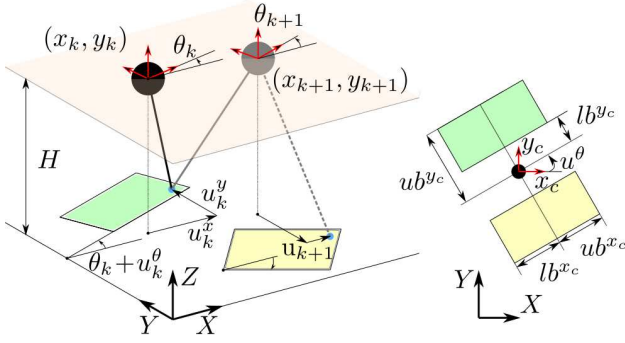


Fig. 2. 3D LIP model with reachability rectangles.

Assuming that each step has a constant time duration T , the step-by-step evolution of the LIP is given by

$$\mathbf{x}_{k+1} = A\mathbf{x}_k + B\mathbf{u}_k \quad (13)$$

where $\mathbf{x}_k = [x_k \ \dot{x}_k \ y_k \ \dot{y}_k \ \theta_k]^\top$ and $\mathbf{u}_k = [u_k^x \ u_k^y \ u_k^\theta]^\top$ are the state and input values at the beginning of the k -th step; the matrices A and B can be found in [11]. To plan motions in the horizontal plane, we define

$$y_k = C\mathbf{x}_k \quad (14)$$

where C is the 2×5 matrix so that $C\mathbf{x} = [x \ y]^\top$.

2) *Constraints*: To ensure that the motions suggested by the LIP are within the capabilities of Digit, we introduce the following constraints. The first constraint captures the reachability rectangles for foot placement and can be described by

$$\text{lb}_k \leq \text{Rot}(\theta_k + u_k^\theta)^\top \mathbf{u}_k \leq \text{ub}_k \quad (15)$$

where $\text{lb}_k = [\text{lb}_k^{x_c} \ \text{lb}_k^{y_c} \ \text{lb}_k^{\theta}]^\top$ (resp. ub_k) includes lower (resp. upper) bounds determining the rectangles, as shown in Fig. 2 and $\text{Rot}(\theta_k + u_k^\theta)$ denotes the 3D rotation matrix about the Z axis by the angle $\theta_k + u_k^\theta$.

To avoid infeasible motions, we introduce a constraint that limits the distance covered by the LIP during each step within the interval $[\delta_{\min}, \delta_{\max}]$ with suitably chosen $0 \leq \delta_{\min} < \delta_{\max}$. Formally, we require

$$\delta_{\min} \leq \sqrt{\Delta x_k^2 + \Delta y_k^2} \leq \delta_{\max} \quad (16)$$

where $\Delta x_k = x_{k+1} - x_k$ and $\Delta y_k = y_{k+1} - y_k$. Note here that when the underlying path has small curvature, (16) has a similar effect with the constraint $v_k \in [0, v_{\max}]$ in (5); however, for paths with considerable curvature, the two constraints influence the system in different ways: (5) limits how far into the path the robot can travel in each step while (16) constrains the Cartesian distance travelled per step.

Finally, obstacles—either static or moving—can be incorporated via additional constraints in the MPC as in [11]. For simplicity, let us consider a circular obstacle of radius r , the location $\mathbf{p}_k^{\text{obs}}$ of which is known at each step k . Collisions can then be avoided by imposing the barrier constraint

$$b(A\mathbf{x}_k + B\mathbf{u}_k) \geq (1 - \gamma)b(\mathbf{x}_k) \quad (17)$$

where the parameter $\gamma \in (0, 1)$ and $b(\mathbf{x}_k) = (C\mathbf{x}_k - \mathbf{p}_k^{\text{obs}})^\top (C\mathbf{x}_k - \mathbf{p}_k^{\text{obs}}) - r^2$. This procedure can be extended to avoid collisions with multiple obstacles and can include obstacles of elliptical shape as well; see [11] for more details.

3) *MPC formulation*: The path tracking MPC program of Section II can be adapted as follows:

$$\begin{aligned} & \underset{X, U, V}{\text{minimize}} && \sum_{\ell=k}^{k+N-1} J_1(\mathbf{x}_\ell, \vartheta_\ell, \mathbf{u}_\ell, \mathbf{v}_\ell) + J_2(\mathbf{x}_{k+N}, \vartheta_{k+N}) \\ & \text{subject to} && \mathbf{x}_k = \mathbf{x}_{\text{init}}, \quad \vartheta_k = \vartheta_{\text{init}} \\ & && \mathbf{x}_{\ell+1} = A\mathbf{x}_\ell + B\mathbf{u}_\ell, \quad \vartheta_{\ell+1} = \vartheta_\ell + \mathbf{v}_\ell \\ & && (\mathbf{x}_\ell, \mathbf{u}_\ell) \in \mathcal{XU}_\ell, \quad \vartheta_\ell \in \Theta, \quad \mathbf{v}_\ell \in \mathcal{V} \\ & && \vartheta_{k+N} \in \Theta \end{aligned}$$

where $\ell = k, \dots, k+N-1$, the cost functions J_1, J_2 are given by (6), (7) with the output $h(\mathbf{x})$ replaced by (14), and

$$\begin{aligned} \mathcal{XU}_\ell = \{ & (\mathbf{x}_\ell, \mathbf{u}_\ell) \mid \text{lb}_\ell \leq \text{Rot}(\theta_\ell + u_\ell^\theta)^\top \mathbf{u}_\ell \leq \text{ub}_\ell, \\ & \text{and } \delta_{\min} \leq \sqrt{\Delta x_\ell^2 + \Delta y_\ell^2} \leq \delta_{\max}, \\ & \text{and } b(A\mathbf{x}_\ell + B\mathbf{u}_\ell) \geq (1 - \gamma)b(\mathbf{x}_\ell) \} \end{aligned}$$

combines the constraints (15)-(17) in a single state- and input-dependent set. The symbols Θ and \mathcal{V} correspond to intervals defined in Section II above. At step k , the MPC requires \mathbf{x}_{init} and ϑ_{init} . The former is available through feedback of the robot's state and the latter is computed by

$$\vartheta_{\text{init}} = \underset{\vartheta}{\text{argmin}} \|C\mathbf{x}_{\text{init}} - \mathbf{y}^d(\vartheta)\|^2 \quad (19)$$

which corresponds to the value of ϑ that minimizes the distance between the robot and the path; i.e., ϑ_{init} is the point on the path closest to the robot's location $C\mathbf{x}_{\text{init}}$.

B. Closing the loop with Digit

The bipedal robot Digit shown in Fig. 3 has a total of 30 Degrees of Freedom (DOF)s; 20 are directly actuated, 4 correspond to leaf springs at the legs and are passive, and 6

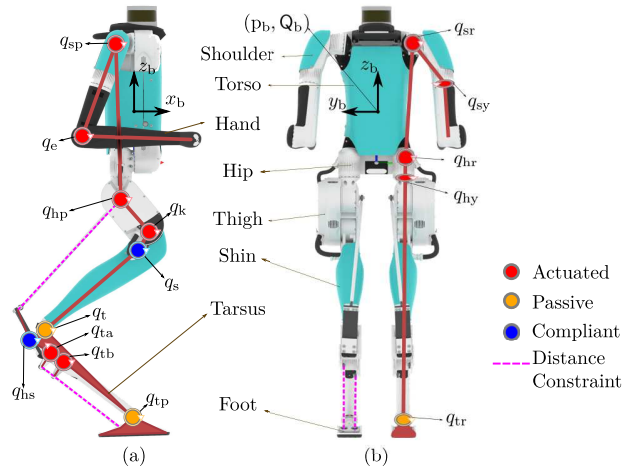


Fig. 3. The bipedal robot Digit and relevant coordinates. (a) Side view; the kinematic loops actuating the tarsus and foot are highlighted with the dotted magenta lines. (b) Back view.

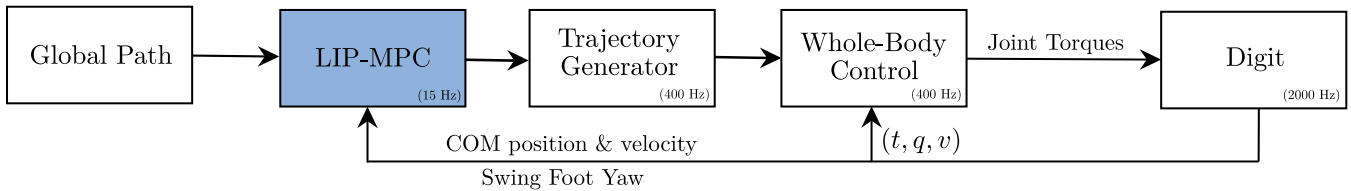


Fig. 4. Implementation of the MPC with Cartesian or contouring error representations on Digit.

represent the position and orientation of a body-fixed frame relative to an inertial frame. The robot with a suitable choice of coordinates is shown in Fig. 3.

The structure of Digit’s controller is shown in Fig. 4. With feedback of Digit’s COM location, velocity and swing foot position and orientation, the initial state x_{init} required by the MPC is then solved as described above to suggest a target footstep location and orientation, and COM position for the next step. The output of the MPC is then fed to the trajectory generator shown in Fig. 4, which uses interpolation to obtain the COM and swing foot position and orientation trajectories for Digit; see [26] for relevant details. These trajectories are then used to define the outputs

$$\begin{bmatrix} (\text{COM Position})_{3 \times 1} \\ (\text{Torso Orientation})_{3 \times 1} \\ (\text{Swing Foot Position})_{3 \times 1} \\ (\text{Swing Foot Orientation})_{3 \times 1} \end{bmatrix}_{12 \times 1}$$

The objective of the QP controller is then to minimize the weighted sum of the square norm of

- the error from the desired outputs computed above;
- the error from a desired constant arm configuration; and
- Digit’s centroidal angular momentum;

while satisfying physical constraints such as torque saturation and contact wrench constraints. Due to space limitations, we do not provide further details on the formulation of the QP here; these can be found in [26].

IV. RESULTS

This section evaluates the method using high-fidelity simulations of the bipedal robot Digit tasked with following a reference path. All simulations are performed using the physics-based simulator MuJoCo [27], with the simulation loop operating at 2kHz. The MPC is programmed in Python using Casadi [28] and solved at 15Hz using interior point solver IPOPT [29]. The average computation time for solving

the MPC including the optimization (19) for v_{init} is 12ms. The low-level QP is formulated using CVXPY [30] and solved at 400Hz with its pre-shipped solver. All computations were carried out on an Intel PC equipped with i7 processor (2.60 GHz) and 16GB RAM. The input weights $R = \text{diag}\{100, 100, 5\}$, the upper bound on the parameter update $v_{\text{max}} = 0.3$ and the horizon $N = 5$ are kept fixed for all cases in this section. Refer to [31] for simulation video.

A. Path Following Performance under Disturbances

We discuss here the performance of the MPCC controller in following curved paths under disturbances; we include results only for a circular path with radius 2m, noting that other curved paths can also be followed with similar performance. Here, the weight matrices for the contouring and lag errors are selected as $\bar{Q} = \bar{W} = \text{diag}\{300, 3\}$ and $\rho = 10$. Figure 5(a) shows the path following performance of the MPC controller without external disturbances and Fig. 5(b) shows the corresponding contouring error, indicating satisfactory tracking performance. On the other hand, Fig. 5(c) shows tracking of the same path under random external disturbances. The disturbances are forces with magnitude sampled from a uniform distribution over the interval $[-50, 50]$ N and are applied at Digit’s torso over a duration of 0.1s at random instants separated by at most 2s. As seen from Fig. 5, the MPCC is able to track the given path even in presence of disturbances with occasional spikes appearing when the disturbances are present.

B. Overtaking Moving Obstacles: A Case Study

We consider here a scenario in which Digit is tasked with following a given path that is shared by a moving obstacle ahead of the robot. We compare two cases: In the first, the objective of the MPC is to minimize the norm of the Cartesian error from the path, while in the second, to minimize the contouring and lag errors corresponding to the MPCC formulation. The goal of this comparison is to demonstrate the benefits of the MPCC, which allows the

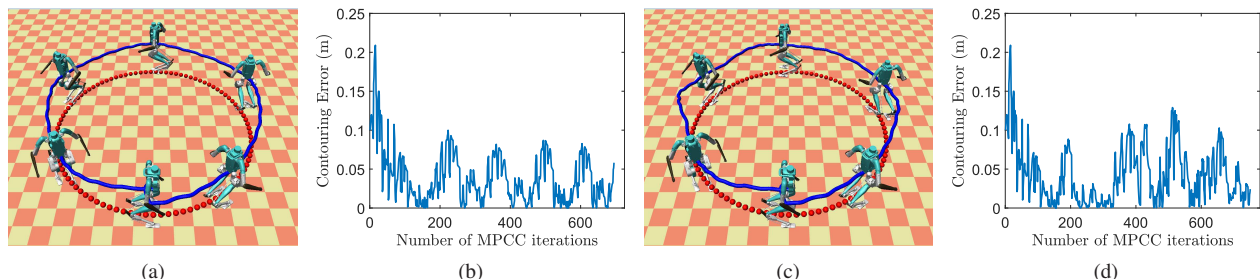


Fig. 5. Tracking performance of the MPCC; the reference path is in red and the robot’s COM path is in blue. (a) Digit follows a circular path with no external disturbances. (b) Contouring error for the case of Fig. 5(a). (c) Digit follows the same path as Fig. 5(a) under randomly applied external disturbances. (d) Corresponding contouring error.

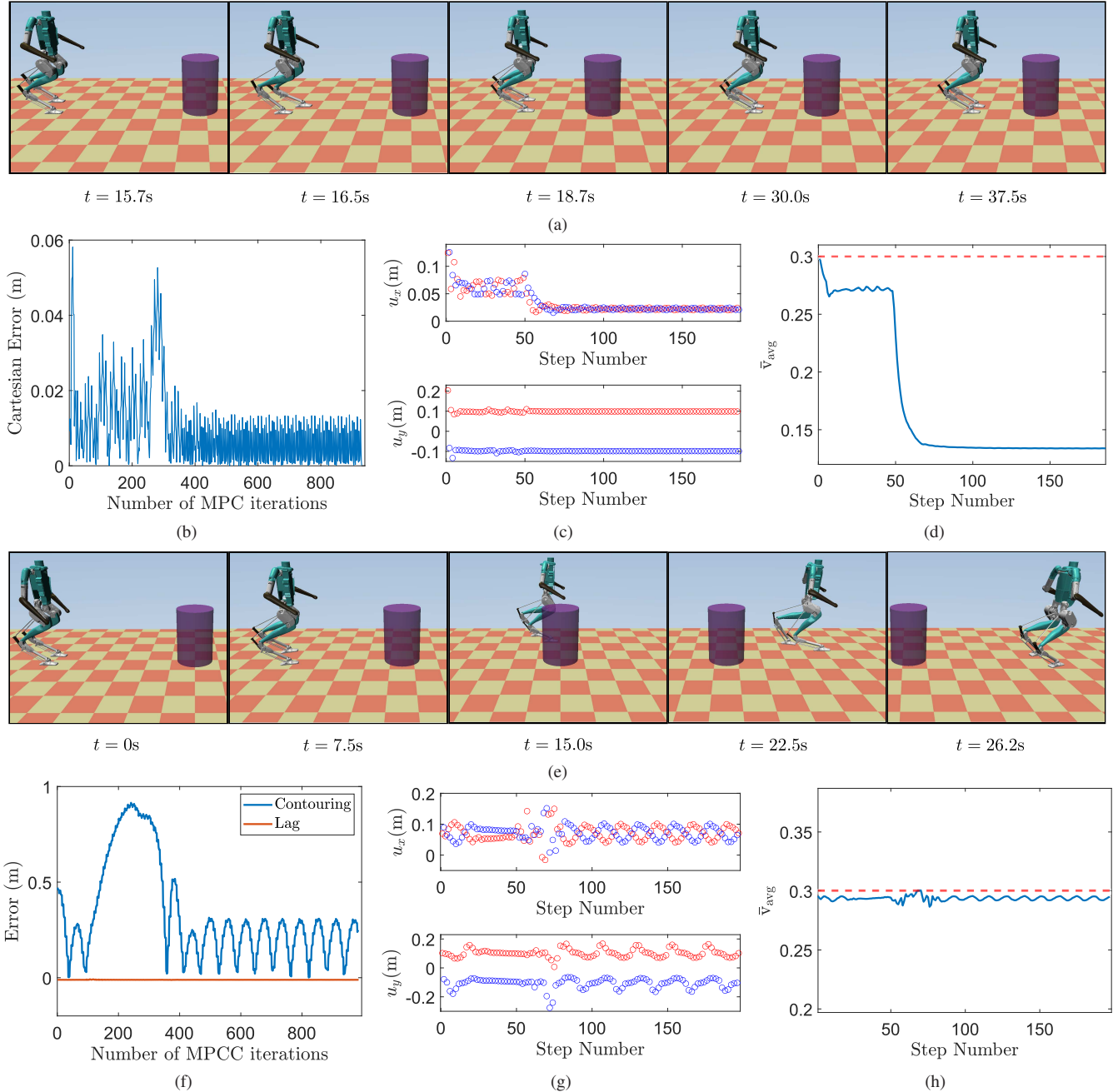


Fig. 6. Cartesian versus contouring error formulations. (a) Digit trailing behind a moving obstacle via Cartesian error MPC. (b) Cartesian error norm. (c) Right (blue) and left (red) footsteps. (d) Average path update parameter (blue) and max value (red). (e) Digit overtaking the moving obstacle via MPCC. (f) Contouring (blue) and lag (red) errors. (g) Right (blue) and left (red) footsteps. (h) Average path update parameter (blue) and max value (red).

robot to decide between emphasizing path following quality versus fast overall path traversal. For simplicity, and without loss of generality, we consider a straight-line path and a cylindrical obstacle with radius $r_{obs} = 0.25m$ moving at constant speed along the path.

In the first case, we assume that the obstacle is moving with a slow speed $0.1m/s$, and we select equal gain matrices $Q = W = 200I$ and $\rho = 50$ in (6)-(7), corresponding to the Cartesian error norm. As we can see from Fig. 6(a), Digit quickly covers the distance from the obstacle, but cannot pass it because the objective of minimizing the Cartesian error norm does not allow temporary deviations from the

path. This is evident from Fig. 6(b), which shows that the norm of the Cartesian error remains below $0.06m$. To keep following the path with high accuracy while avoiding collisions with the obstacle, Digit adjusts its stepping online to take shorter steps; this can be seen in Fig. 6(c), where the step size u^x along the X direction decreases when the obstacle constraint is activated. As a measure of how “deep” into the path the robot moves, Fig. 6(d) presents the average path update parameter $\bar{v}_{avg} = (1/N) \sum_{\ell=0}^{N-1} v_{\ell}$ over the horizon N for each iteration of the MPC. The obstacle constraint prevents the MPC from suggesting large updates

in the path parameter.

For the MPCC, the obstacle is moving at a higher speed 0.6m/s, comparable with Digit's speed. Here, the weight matrices are $\bar{Q} = \bar{W} = \text{diag}\{1, 1000\}$ and $\rho = 50$. This choice emphasizes the lag component of the cost over the contouring component; thus, the controller is more tolerant to deviations from the path, prioritizing fast overall path traversal. It can be seen from Fig. 6(e) that Digit overtakes the moving obstacle. This is achieved because, as shown in Fig. 6(f), the controller allows the robot to temporarily deviate from the path—the contouring error increases—while the lag error is kept almost zero. It is clear from Fig. 6(g) that the stepping size of the robot increases in the X direction, while small deviations in the Y direction allow Digit to skirt around the obstacle and eventually leave it behind. This behavior is due to the larger weight chosen for the lag component of the error, as compared to the contouring component. From Fig. 6(h), we can see that the MPCC constantly keeps the parameter v_{avg} close to the maximum bound v_{max} , thus encouraging the robot to go as far into the path as the MPCC constraints allow.

V. CONCLUSION

This paper presented a MPCC scheme for foot placement that enables bipedal robots to make online decisions on the speed and accuracy with which they follow a planned global path. Unlike other approaches, the proposed method does not require specifying a feasible trajectory or a speed profile in advance. Using physics-based simulations with the bipedal robot Digit, we discussed aspects of MPCC that allow temporary deviations from the reference path to favor fast traversal of the overall path. We demonstrated these capabilities in the case where Digit overtakes a moving obstacle that shares its path. Our future work will focus on experimentally validating the proposed approach and on integrating MPCC with safe walking corridors [11] to ensure fast path traversal and safety in highly-cluttered spaces.

REFERENCES

- [1] R. Tedrake, S. Kuindersma, R. Deits, and K. Miura, "A closed-form solution for real-time ZMP gait generation and feedback stabilization," in *Proc. IEEE Int. Conf. Humanoid Robots*, 2015, pp. 936–940.
- [2] J. Alcaraz-Jiménez, D. Herrero-Pérez, and H. Martínez-Barberá, "Robust feedback control of ZMP-based gait for the humanoid robot Nao," *Int. J. Robot. Res.*, vol. 32, no. 9-10, pp. 1074–1088, 2013.
- [3] S. Faraji, S. Pouya, and A. Ijspeert, "Robust and agile 3D biped walking with steering capability using a footstep predictive approach," in *Proc. Robot. Sci. Syst.*, 2014.
- [4] A. Tanguy, D. De Simone, A. I. Comport, G. Oriolo, and A. Kheddar, "Closed-loop MPC with dense visual SLAM - stability through reactive stepping," in *Proc. IEEE Int. Conf. Robot. Autom.*, 2019, pp. 1397–1403.
- [5] S. Xin, R. Orsolino, and N. Tsagarakis, "Online relative footstep optimization for legged robots dynamic walking using discrete-time model predictive control," in *Proc. IEEE/RSJ Int. Conf. Intell. Robots Syst.*, 2019, pp. 513–520.
- [6] N. Scianca, D. De Simone, L. Lanari, and G. Oriolo, "MPC for humanoid gait generation: Stability and feasibility," *IEEE Trans. Robot.*, vol. 36, no. 4, pp. 1171–1188, 2020.
- [7] S. Kajita, F. Kanehiro, K. Kaneko, K. Yokoi, and H. Hirukawa, "The 3D linear inverted pendulum mode: a simple modeling for a biped walking pattern generation," in *Proc. IEEE/RSJ Int. Conf. Intell. Robots Syst.*, 2001, pp. 239–246.
- [8] H. Choset, K. Lynch, S. Hutchinson, G. Kantor, W. Burgard, L. E. Kavraki, and S. Thrun, *Principles of Robot Motion: Theory, Algorithms, and Implementation*. MIT Press, 2005.
- [9] A. Agrawal and K. Sreenath, "Discrete control barrier functions for safety-critical control of discrete systems with application to bipedal robot navigation," in *Proc. Robot. Sci. Syst.*, 2017.
- [10] S. Teng, Y. Gong, J. W. Grizzle, and M. Ghaffari, "Toward safety-aware informative motion planning for legged robots," *arXiv:2103.14252*, 2021.
- [11] K. S. Narkhede, A. M. Kulkarni, D. A. Thanki, and I. Poulakakis, "A sequential MPC approach to reactive planning for bipedal robots using safe corridors in highly cluttered environments," *IEEE Robot. Automat. Lett.*, vol. 7, no. 4, pp. 11 831–11 838, 2022.
- [12] M. S. Motahar, S. Veer, and I. Poulakakis, "Composing limit cycles for motion planning of 3D bipedal walkers," in *Proc. IEEE Conf. Decis. Control*, 2016, pp. 6368–6374.
- [13] S. Veer, M. S. Motahar, and I. Poulakakis, "Almost driftless navigation of 3D limit-cycle walking bipeds," in *Proc. IEEE/RSJ Int. Conf. Intell. Robots Syst.*, 2017, pp. 5025–5030.
- [14] K. S. Narkhede, M. S. Motahar, S. Veer, and I. Poulakakis, "Reactive gait composition with stability: Dynamic walking amidst static and moving obstacles," *arXiv:2303.16165*, 2023.
- [15] S. Veer and I. Poulakakis, "Switched systems with multiple equilibria under disturbances: Boundedness and practical stability," *IEEE Trans. Autom. Control*, vol. 65, no. 6, pp. 2371–2386, 2020.
- [16] Y. Gu, B. Yao, and C. S. George Lee, "Straight-line contouring control of fully actuated 3-D bipedal robotic walking," in *Proc. Amer. Control Conf.*, 2018, pp. 2108–2113.
- [17] Y. Gao and Y. Gu, "Global-position tracking control of a fully actuated NAO bipedal walking robot," in *Proc. Amer. Control Conf.*, 2019, pp. 4596–4601.
- [18] X. Xiong, J. Reher, and A. D. Ames, "Global position control on underactuated bipedal robots: Step-to-step dynamics approximation for step planning," in *Proc. IEEE Int. Conf. Robot. Autom.*, 2021, pp. 2825–2831.
- [19] H. Atsuta, H. Nozaki, and T. Sugihara, "Smooth-path-tracking control of a biped robot at variable speed based on dynamics morphing," in *Proc. IEEE Int. Conf. Robot. Autom.*, 2017, pp. 4116–4121.
- [20] Z. Li, J. Zeng, S. Chen, and K. Sreenath, "Autonomous navigation of underactuated bipedal robots in height-constrained environments," *Int. J. Robot. Res.*, 2023, early access, doi: 10.1177/02783649231187670.
- [21] T. Faulwasser, B. Kern, and R. Findeisen, "Model predictive path-following for constrained nonlinear systems," in *Proc. IEEE Conf. Decis. Control*, 2009, pp. 8642–8647.
- [22] D. Lam, C. Manzie, and M. Good, "Model predictive contouring control," in *Proc. IEEE Conf. Decis. Control*, 2010, pp. 6137–6142.
- [23] L. Tang and R. G. Landers, "Predictive contour control with adaptive feed rate," *IEEE/ASME Trans. Mechatronics*, vol. 17, no. 4, pp. 669–679, 2012.
- [24] B. Brito, B. Floor, L. Ferranti, and J. Alonso-Mora, "Model predictive contouring control for collision avoidance in unstructured dynamic environments," *IEEE Robot. Automat. Lett.*, vol. 4, no. 4, pp. 4459–4466, 2019.
- [25] J. Ji, X. Zhou, C. Xu, and F. Gao, "CMPCC: Corridor-based model predictive contouring control for aggressive drone flight," in *Proc. Int. Symp. Exp. Robot.*, 2020, p. 37–46.
- [26] K. S. Narkhede, A. M. Kulkarni, D. A. Thanki, and I. Poulakakis, "A sequential MPC approach to reactive planning for bipedal robots," *arXiv:2205.00156*, 2022.
- [27] E. Todorov, T. Erez, and Y. Tassa, "MuJoCo: A physics engine for model-based control," in *Proc. IEEE/RSJ Int. Conf. Intell. Robots Syst.*, 2012, pp. 5026–5033.
- [28] J. A. E. Andersson, J. Gillis, G. Horn, J. B. Rawlings, and M. Diehl, "CasADi-A software framework for nonlinear optimization and optimal control," *Math. Program. Comput.*, vol. 11, no. 1, pp. 1–36, 2019.
- [29] A. Wächter and L. T. Biegler, "On the implementation of an interior-point filter line-search algorithm for large-scale nonlinear programming," *Math. Program.*, vol. 106, pp. 25–57, 2006.
- [30] S. Diamond and S. Boyd, "CVXPY: A Python-embedded modeling language for convex optimization," *J. Mach. Learn. Res.*, vol. 17, no. 83, pp. 1–5, 2016.
- [31] Simulation results. [Online]. Available: <https://youtu.be/5FBwor9ROK4>